

## Scaling analysis of quasiperiodic systems: Generalized Harper model

Hisashi Hiramoto

*Institute of Materials Science, University of Tsukuba, Tsukuba, Ibaraki 305, Japan*

Mahito Kohmoto

*Institute for Solid State Physics, University of Tokyo, 7-22-1 Roppongi, Minato-ku, Tokyo 106, Japan  
and Department of Physics, University of Utah, Salt Lake City, Utah 84112*

(Received 7 March 1989; revised manuscript received 26 June 1989)

Properties of one-dimensional quasiperiodic discrete Schrödinger equations are analyzed by means of a finite-size scaling of the spectrum and the wave function. The incommensurate Harper model, which has only one Fourier component in the potential, is analyzed as an example, and some quantitative results, which are consistent with previously known qualitative features, are obtained. In addition, some universal behaviors are observed. The methods are also applied to a generalized model with the potential having two Fourier components. The existence of mobility edges is demonstrated and the phase diagram on localized and extended states is shown.

### I. INTRODUCTION

An electron (or a phonon) in quasiperiodic (QP) systems is a subject of great interest. In such systems, the wave functions and the spectra exhibit all the possibilities:<sup>1</sup> localized wave functions (dense point spectrum), extended wave functions (absolutely continuous spectrum), and critical wave functions (singular continuous spectrum). Various QP models have been studied so far in terms of various analytical or numerical techniques. In particular, a number of investigations have been made for a one-dimensional tight-binding model:

$$-\psi_{n+1} - \psi_{n-1} + V(\omega n + \theta)\psi_n = E\psi_n, \quad (1)$$

where  $V(x)$  is a periodic function with periodic 1 [ $V(x+1) = V(x)$ ],  $\omega$  is an irrational number, and  $\theta$  is a phase constant.

For several forms of  $V(x)$ , the properties of the wave functions and the spectra have been well understood. The model defined by<sup>2-6</sup>

$$V(x) = \lambda \cos(2\pi x), \quad (2)$$

which is known as the Harper model, undergoes a metal-insulator transition at  $\lambda = 2$ .<sup>4</sup> That is, for  $\lambda < 2$ , all the states are extended, while for  $\lambda > 2$ , all the states are localized. At  $\lambda = 2$ , all the states are critical.

In the model defined by<sup>7</sup>

$$V(x) = \lambda \tan(2\pi x), \quad (3)$$

on the other hand, all the states are localized for any value of  $\lambda$ . This is presumably due to the unboundedness of the potential.

Another well-known one-dimensional QP tight-binding model is the Fibonacci model,<sup>8,9</sup> which is defined by  $\omega = \sigma \equiv (\sqrt{5} - 1)/2$  (the reciprocal of the "golden mean") and

$$V(x) = \begin{cases} -\lambda, & m - \sigma < x \leq m \\ \lambda, & m < x \leq m + 1 - \sigma \end{cases} \quad (4)$$

where  $m$  stands for arbitrary integers. In this model, all the states are critical, irrespective of  $\lambda$ .

The above models have a common feature: the spectrum is pure at each value of  $\lambda$ , i.e., extended, localized, and critical states do not coexist in a spectrum, and there are no mobility edges. However, there is no *a priori* reason why all QP models have a pure spectrum; thus they may have mobility edges. In fact, the existence of mobility edges has been previously suggested for the generalized Harper model, where two Fourier components are contained in  $V(x)$ .<sup>4,10,11</sup> We have recently reported novel behavior of mobility edges in the model.<sup>12</sup>

$$V(x) = \lambda \tanh[\mu \cos(2\pi x)] / \tanh \mu, \quad (5)$$

in which localization could take place from the center of the spectrum as  $\lambda$  is increased.

If the spectrum is nonpure and mobility edges exist in a QP model, the next question is the structure of the mobility edges in the spectrum. In general, the band structure of one-dimensional QP systems is infinitely nesting, and has infinitely many gaps. From that, one possibility is that there would be infinitely many mobility edges.<sup>4</sup> As for model (5), we showed that this is not the case, and that only a finite number of mobility edges exist.<sup>12</sup> In this paper, we show that the generalized Harper model also has a finite number of mobility edges.

When one studies Eq. (1) numerically, an irrational number  $\omega$  must be approximated by a rational approximant. In order to determine whether the states of a model are extended, localized, or critical, a series of rational approximants converging to the irrational  $\omega$  is taken; then the asymptotic dependence of the spectrum or the wave function on the approximants in the series is studied. For a model with a pure spectrum, one can distinguish extended, localized, and critical states by measuring the total bandwidth of the spectrum.<sup>4,5</sup> A multifractal analysis of the spectrum in the critical case also works well in such cases.<sup>13</sup> In the nonpure case, however, individual states in the spectrum have to be studied. In

studying model (5), we used two methods of analysis: one is the study of an asymptotic behavior of the bandwidths corresponding to the individual states; the other is a multifractal analysis of wave functions themselves. In this paper, we explain in detail the methods which were briefly sketched in Ref. 12, and apply them to the Harper model and the generalized Harper model.

The remainder of this paper is organized as follows. In Sec. II, the methods of the analysis are presented. In Sec. III, the methods are applied to the Harper model [Eq. (2)], and it is demonstrated how clearly one can distinguish extended, localized, and critical states through the methods. In Sec. IV, the model with  $V(x)$  containing two Fourier components is studied in detail, and the mobility-edge structure is exhibited. A summary and conclusions are given in Sec. V.

## II. METHODS

The rational approximants for  $\omega$  are obtained by the continued-fraction expansion for  $\omega$ . For a rational approximant  $M/N$ , the system is periodic; thus the spectrum consists of a finite number of bands. When going to the next approximation step, each band splits into several subbands. Thus the spectrum for the irrational  $\omega$  has infinitely many band gaps, and has a hierarchical structure. In the Fibonacci model, this hierarchical structure in fact has scaling, which can be explained by analysis of an exact renormalization-group transformation.<sup>14</sup>

### A. Scaling analysis of bandwidths

One method to determine whether a state is extended, localized, or critical is to study the dependence of the bandwidth on  $N$ . If the state is localized, the bandwidth  $B$  should decrease exponentially as  $N$  is increased. If the state is extended or critical, on the other hand,  $B$  is expected to behave as

$$B \sim 1/N^\gamma. \quad (6)$$

When the state is extended,  $\gamma$  is 1 for almost all the cases. However, there exist extended states with  $\gamma=2$ .<sup>13</sup> These states correspond to "band edges" and the behavior comes from a remnant of Van Hove singularity in one-dimensional bands. This point will further be discussed in the next section with an example in the Harper model. When the state is critical,  $\gamma$  can take a value greater than 1. In fact, the distribution of  $\gamma$  ( $\alpha \equiv 1/\gamma$ ) in the whole spectrum has been studied from a multifractal point of view for the Harper model with the critical coupling<sup>13</sup> and the Fibonacci model<sup>15</sup> in which all the states are critical irrespective of the coupling.

### B. Multifractal analysis of wave functions

Another method of analysis is to study a wave function itself. Now let the  $n$ th approximant for  $\omega$  be  $M/N$ . Then the system is periodic with period  $N$ . A wave function is analyzed as a set on lattice sites with probability measure

$$p_j = |\psi_j|^2 \quad (j=1, 2, \dots, N), \quad (7)$$

where the probability measure is normalized to unity ( $\sum_{j=1}^N p_j = \sum_{j=1}^N |\psi_j|^2 = 1$ ). We assign a Lebesgue measure  $l=1/N$  to all the sites. Thus the probability measure is supported by an interval  $[0,1]$  for each stage of approximation. We study the  $n \rightarrow \infty$  behavior of the set from a multifractal point of view.<sup>16</sup> Since we have taken a uniform Lebesgue measure, the scaling index  $\epsilon$  defined by  $l \sim \exp(-\epsilon n)$  has no distribution. The scaling index of the probability measure  $\alpha$  studied here is defined by

$$p_j \sim l^{\alpha_j} = (1/N)^{\alpha_j}. \quad (8)$$

We study the singular spectrum  $f(\alpha)$  defined by  $\Omega(\alpha) \sim l^{-f(\alpha)}$ , where  $\Omega(\alpha)d\alpha$  is the number of lattice points having  $\alpha$  between  $\alpha$  and  $\alpha+d\alpha$ . For extended wave functions, the probability measure scales as  $p_j \sim 1/N=l$ ; thus  $f(\alpha)$  is defined only at  $\alpha=1$  [ $f(1)=1$ ]. For localized wave functions, on the other hand,  $p_j$  is finite ( $\alpha=0$ ) only on a finite number of lattice points and is exponentially small ( $\alpha=\infty$ ) on the other points; thus  $f(\alpha)$  is defined at  $\alpha=0$  [ $f(0)=0$ ] and  $\alpha=\infty$  [ $f(\infty)=1$ ]. For critical wave functions,  $\alpha$  has a distribution, i.e.,  $f(\alpha)$  is a smooth function defined on a finite interval  $[\alpha_{\min}, \alpha_{\max}]$ .

The multifractal analysis of the wave functions in one-dimensional QP models has already been tried by several workers.<sup>17-21</sup> We calculate  $f(\alpha)$  or equivalently the entropy function  $S(\alpha)$ , following the method developed in Refs. 16, 22, and 17. The entropy function can be calculated by an analogous formalism to the usual statistical mechanics. First we introduce a free energy defined by

$$G(q) = \lim_{n \rightarrow \infty} G_n(q), \quad (9)$$

where

$$G_n(q) = \frac{1}{n} \ln Z_n(q), \quad (10)$$

and

$$Z_n(q) = \sum_{j=1}^N p_j^q. \quad (11)$$

The entropy function is obtained through the Legendre transformation as

$$S(\alpha) = G(q) + \epsilon \alpha q, \quad (12)$$

and

$$\alpha = -\frac{1}{\epsilon} \frac{dG(q)}{dq}. \quad (13)$$

The entropy function  $S(\alpha)$  and the singular spectrum  $f(\alpha)$  relate with each other as

$$S(\alpha) = \epsilon f(\alpha). \quad (14)$$

When we make a numerical analysis following the above formalism, we have to be deliberate on the finite-size effect. If we calculate  $f(\alpha)$  from Eqs. (12) and (13) by replacing  $G(q)$  by  $G_n(q)$  with a finite  $n$ , the obtained  $f(\alpha)$  is a smooth function of  $\alpha$ , irrespective of the wave function being extended, localized, or critical. However,  $f(\alpha)$  is smooth only for critical wave functions. There-

fore, in order to distinguish localized, extended, or critical states, one has to obtain  $G(q)$  by a careful extrapolation from  $G_n(q)$  with finite  $n$ 's before applying the Legendre transformation [Eqs. (12) and (13)]. From Eqs. (9)–(11), it is expected that

$$G_n(q) \sim G(q) + O(1/n). \quad (15)$$

Thus we should plot  $G_n(q)$  against  $1/n$  for every value of  $q$ , and estimate  $G(q)$  in a limit  $1/n \rightarrow 0$ .

In practice, we can distinguish localized, extended, and critical states by studying only the asymptotic behaviors of  $G_n(q)$  in  $q \rightarrow \pm\infty$ . When  $f(\alpha)$  has nonzero values only on  $[\alpha_{\min}, \alpha_{\max}]$ , there exist constants  $q_c$  and  $q_c'$  such that if  $q > q_c$  or  $q < q_c'$ ,  $G(q)$  is linear with respect to  $q$ :

$$G(q) = \begin{cases} \epsilon(f_{\min} - \alpha_{\min}q), & q > q_c \\ \epsilon(f_{\max} - \alpha_{\max}q), & q < q_c' \end{cases} \quad (16)$$

where  $f_{\min} = f(\alpha_{\min})$  and  $f_{\max} = f(\alpha_{\max})$ . If  $\partial f / \partial \alpha|_{\alpha \rightarrow \alpha_{\max} + 0} = \infty$  ( $\partial f / \partial \alpha|_{\alpha \rightarrow \alpha_{\min} - 0} = -\infty$ ),  $q_c$  ( $q_c'$ ) goes to  $\infty$  ( $-\infty$ ); then Eq. (16) holds only asymptotically. In any case, by studying the asymptotic behaviors of  $G_n(q)$ :

$$G_n(q) \sim \begin{cases} \epsilon(f_{\max}^{(n)} - \alpha_{\max}^{(n)}q) & \text{as } q \rightarrow -\infty, \\ \epsilon(f_{\min}^{(n)} - \alpha_{\min}^{(n)}q) & \text{as } q \rightarrow +\infty, \end{cases} \quad (17)$$

we can obtain  $\alpha_{\min}$ ,  $\alpha_{\max}$ ,  $f(\alpha_{\min})$ , and  $f(\alpha_{\max})$  through the relations

$$\begin{aligned} \alpha_{\min} &= \lim_{n \rightarrow \infty} \alpha_{\min}^{(n)}, \\ \alpha_{\max} &= \lim_{n \rightarrow \infty} \alpha_{\max}^{(n)}, \\ f(\alpha_{\min}) &= \lim_{n \rightarrow \infty} f_{\min}^{(n)}, \\ f(\alpha_{\max}) &= \lim_{n \rightarrow \infty} f_{\max}^{(n)}. \end{aligned} \quad (18)$$

When a wave function is critical,  $\alpha_{\min}$  and  $\alpha_{\max}$  should have different finite values. When a wave function is extended, namely when  $f(\alpha)$  is defined only at  $\alpha=1$  and  $f(1)=1$ , one should obtain the results  $\alpha_{\min} = \alpha_{\max} = 1$  and  $f(\alpha_{\min}) = f(\alpha_{\max}) = 1$ . When a wave function is localized, one should obtain the results  $\alpha_{\min} = 0$ ,  $\alpha_{\max} = \infty$ ,  $f(\alpha_{\min}) = 0$ , and  $f(\alpha_{\max}) = 1$ . In the following sections, we first estimate  $\alpha_{\min}$ ,  $\alpha_{\max}$ ,  $f(\alpha_{\min})$ , and  $f(\alpha_{\max})$  from (17) and (18), and determine whether a wave function is extended, localized, or critical; then only when the wave function is critical, we calculate a whole curve of  $f(\alpha)$ .

Finally, in this section, we discuss the relation between this extrapolation and a technique often used in the standard formalism for  $f(\alpha)$ .<sup>16</sup> In the standard formalism,  $\tau(q)$  defined by

$$\lim_{n \rightarrow \infty} \Gamma_n(q, \tau) = 1 \quad (19)$$

is introduced. Here  $\Gamma_n(q, \tau)$  is defined by

$$\Gamma_n(q, \tau) = N^\tau Z_n(q), \quad (20)$$

although a generalization is required when the set ana-

lyzed has a distribution of Lebesgue measure. The singular spectrum  $f(\alpha)$  can be obtained from  $\tau(q)$  through a Legendre transformation. In place of solving Eq. (19),  $\tau(q)$  is often calculated numerically from

$$\Gamma_n(q, \tau) / \Gamma_{n'}(q, \tau) = 1, \quad n \neq n'. \quad (21)$$

This procedure is a sort of extrapolation. This corresponds to assuming that  $G_n - G = \text{const}/n$ . However, the prefactor of  $1/n$  may oscillate. In fact, we will find such a situation in the next section.

### III. APPLICATION TO THE HARPER MODEL

From now on, we take  $\omega$  to be  $\sigma = (\sqrt{5}-1)/2$  (the reciprocal of the golden mean). The rational approximants for  $\sigma$  are  $F_{n-1}/F_n$ , where  $F_n$  is the  $n$ th Fibonacci number defined by  $F_n = F_{n-1} + F_{n-2}$  with  $n \geq 2$ , and  $F_0 = F_1 = 1$ . Since  $F_{n-1}/F_n \sim \sigma = (\sqrt{5}-1)/2$ , as  $n \rightarrow \infty$ , the scaling index of the Lebesgue measure,  $\epsilon$ , is  $\ln(1/\sigma)$ . In this case, each band splits into three subbands as  $n$  is increased. Therefore, each point in the spectrum for the irrational limit ( $n \rightarrow \infty$ ) is specified by an infinite sequence of 1, 0, and  $\bar{1}$ , which represent the upper, middle, and lower subbands, respectively.<sup>15</sup> Therefore, the procedure one needs to carry out to analyze the properties of the state specified by a sequence is to study the asymptotic behavior of the wave function or the bandwidth along the sequence.

In this section, we analyze the spectrum and the wave functions of the Harper model defined by Eqs. (1) and (2). Here the phase constant  $\theta$  in Eq. (1) is taken to be 0. In this model, we encounter all the possible states: extended, localized, and critical. We demonstrate how clearly one can distinguish whether a state in the spectrum is extended, localized, or critical.

#### A. Scaling analysis of bandwidths

First, we carry out the bandwidth analysis. When the state under the investigation is specified by an infinite sequence  $\{C_1 C_2 C_3 C_4 C_5 C_6 \cdots\}$  ( $C_j = 1, 0, \text{ or } \bar{1}$ ), we measure the width ( $B_n$ ) of the band specified by a finite subsequence  $\{C_1 C_2 C_3 \cdots C_q\}$ , which is a band of a periodic system with period  $N = F_n$ . Then the relation between  $B_n$  and  $F_n$  is traced. Figure 1 is plots of  $F_n B_n$  versus  $n$  [ $\approx \ln F_n / \ln(1/\sigma)$ ] for several states with (a)  $\lambda = 1.9$ , (b)  $\lambda = 2.0$ , and (c)  $\lambda = 2.1$ . The states displayed in this figure are (1)  $\{000000 \cdots\}$ , (2)  $\{\bar{1}\bar{1}\bar{1}\bar{1}\bar{1}\bar{1}\}$ , (3)  $\{0\bar{1}\bar{1}\bar{1}\bar{1}\bar{1}\bar{1} \cdots\}$ , (4)  $\{\bar{1}00000 \cdots\}$ , and (5)  $\{\bar{1}0\bar{1}0\bar{1}0\bar{1}0\bar{1}0 \cdots\}$ .

For  $\lambda = 1.9$ , it is observed that  $F_n B_n \sim 1$  for (1), (4), and (5), while  $F_n B_n \sim 1/F_n$  for (2) and (3). The states (2) and (3) coincide with "edge states" which are in general identified by  $\{\cdots 111111 \cdots\}$  or  $\{\cdots \bar{1}\bar{1}\bar{1}\bar{1}\bar{1}\bar{1} \cdots\}$ . That is,  $\gamma$  in Eq. (6) is 2 if the state is an "edge state," while  $\gamma$  is 1 otherwise. Thus it can be concluded that all the states are extended. This result is consistent with a conjecture that all the states are extended if  $\lambda < 2$ .

For  $\lambda = 2.0$ , the situation is quite different. It is observed that  $B_n \sim (1/F_n)^\gamma$ , where  $\gamma = 1.829$  for (1) and (4);  $\gamma = 2.374$  for (2) and (3);  $\gamma = 1.951$  for (5). This result is

consistent with a conjecture that all the states are critical at  $\lambda=2$ . Here is a point to be noted. The states (1) and (4) are governed by the same index, and the states (2) and (3) are also governed by the same index. By investigating other states, we can conclude that all of the states specified by  $\{\cdots 000000\cdots\}$  (the “center states”) have an identical value of  $\gamma$  ( $=\gamma_C \equiv 1.829$ ), and all of the “edge states” have an identical value of  $\gamma$  ( $=\gamma_E \equiv 2.374$ ) as well. This situation is of the same as the Fibonacci

model, where it can be understood in terms of the exact renormalization group.<sup>14,15</sup> For the state (5),  $\gamma$  takes a value between  $\gamma_C$  and  $\gamma_E$ . In fact,  $\gamma_C$  and  $\gamma_E$  are the minimum and the maximum values of  $\gamma$ , and the distribution of  $\gamma$  (or  $\alpha$  defined by  $1/\gamma$ ) has been studied by a multifractal approach.<sup>13</sup>

The fact that all the “edge states” and the “center states” have identical values of  $\gamma$  ( $\gamma_E$  and  $\gamma_C$ ) suggests the existence of a renormalization-group structure in the Harper model. In fact, Ostlund and Pandit<sup>6</sup> followed this direction in the Harper model.

For  $\lambda=2.1$ ,  $B_n$  is observed to decrease rapidly for all the states; thus localization of all the states can be concluded consistently with a conjecture that all the states are localized for  $\lambda > 2$ .

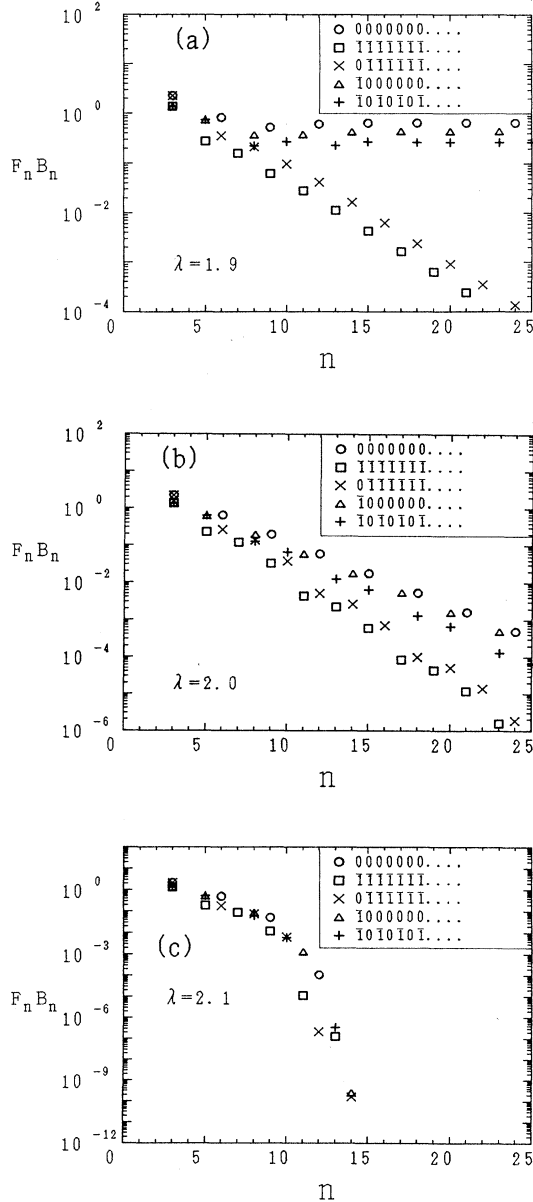


FIG. 1. Plots of  $F_n B_n$  against  $n$  for several states when (a)  $\lambda=1.9$ , (b)  $\lambda=2.0$ , and (c)  $\lambda=2.1$ . In (a), all the states are extended, and in (c), all the states are localized. In (b), all the states are critical; then the values of  $\gamma$  [ $B_n \sim (1/F_n)^\gamma$ ] are 1.829 for the states  $\{\cdots 000000\cdots\}$ , 2.374 for the states  $\{\cdots 111111\cdots\}$ , and 1.961 for the state  $\{10101010\cdots\}$ .

### B. Multifractal analysis of wave functions

Next, we study the wave functions themselves from a multifractal point of view. Before going to the multifractal analysis, we show the wave functions calculated for a finite-size system ( $n=21$ , i.e.,  $N=F_{21}=17711$ ). Although the pictures of the wave functions are found in some previous literature (for example, Ref. 6), it would be instructive to show them here. In Fig. 2, the wave function corresponding to the spectrum edge  $\{\bar{1}\bar{1}\bar{1}\bar{1}\bar{1}\cdots\bar{1}\}$  is displayed for (a)  $\lambda=1.9$ , (b)  $\lambda=2.0$ , and (c)  $\lambda=2.1$ . Also, the wave function corresponding to the center of the spectrum  $\{000000\cdots\}$  is displayed in Fig. 3. From these figures, it may be obvious that the wave functions are extended for  $\lambda=1.9$  and are localized for  $\lambda=2.1$ , although the following analysis is necessary in order to get a convincing conclusion. Furthermore, a character of the wave functions of  $\lambda=2$  is not trivial in itself.

Figure 4 shows a plot of  $G_n(q)$  defined by Eqs. (10) and (11) with  $n=21$  for the state specified by  $\{\bar{1}\bar{1}\bar{1}\bar{1}\bar{1}\bar{1}\bar{1}\cdots\bar{1}\}$ . By calculating  $G_n$  for several values of  $n$ , we estimate the  $n \rightarrow \infty$  limit.

In Fig. 5(a), we plot  $\alpha_{\min}^{(n)}$  against  $1/n$  for  $\lambda=1.9, 2.0$ , and  $2.1$ . By extrapolation, we can estimate the  $n \rightarrow \infty$  limits as  $\alpha_{\min}=1$  for  $\lambda=1.9$ ,  $\alpha_{\min}=0.168$  for  $\lambda=2.0$ , and  $\alpha_{\min}=0$  for  $\lambda=2.1$ . This value of  $\alpha_{\min}$  for  $\lambda=2.0$  is consistent with a previous study.<sup>23</sup> It is observed that the overall behavior of  $\alpha_{\min}^{(n)}$  is linear with respect to  $1/n$ , although it also contains an oscillatory structure. We can also estimate  $\alpha_{\max}$  in terms of a similar analysis as  $\alpha_{\max}=1=\alpha_{\min}$  for  $\lambda=1.9$ ,  $\alpha_{\max}=1.53$  for  $\lambda=2.0$ , and  $\alpha_{\max}=\infty$  for  $\lambda=2.1$ .

In Fig. 5(b), we plot  $f_{\min}^{(n)}$  against  $1/n$ . From this, we can estimate  $f(\alpha_{\min})$  as  $f(\alpha_{\min})=1$  for  $\lambda=1.9$ ,  $f(\alpha_{\min})=0$  for  $\lambda=2.0$ , and  $f(\alpha_{\min})=0$  for  $\lambda=2.1$ . From a similar analysis, we can estimate  $f(\alpha_{\max})$  as  $f(\alpha_{\max})=1=f(\alpha_{\min})$  for  $\lambda=1.9$ ,  $f(\alpha_{\max})=0.77$  for  $\lambda=2.0$ , and  $f(\alpha_{\max})=1$  for  $\lambda=2.1$ .

From the results, we can conclude that the edge state ( $\{\bar{1}\bar{1}\bar{1}\bar{1}\bar{1}\bar{1}\cdots\bar{1}\}$ ) is extended for  $\lambda=1.9$ , critical for  $\lambda=2.0$ , and localized for  $\lambda=2.1$ . The same conclusion can be obtained for the state specified by  $\{000000\cdots\}$ .

Next we show  $f(\alpha)$  for the critical case ( $\lambda=2.0$ ). Figure 6(a) is a plot of  $f(\alpha)$  for  $\{\bar{1}\bar{1}\bar{1}\bar{1}\bar{1}\bar{1}\cdots\bar{1}\}$ . For this

state, the convergence of our numerical estimate is fairly good on the whole range of  $[\alpha_{\min}, \alpha_{\max}]$ . The most probable value of  $\alpha$  ( $\alpha_0$ ), namely  $\alpha$  where  $f(\alpha)$  is maximal [ $f(\alpha)=1$ ], is 1.27. Recently Fujiwara *et al.*<sup>21</sup> calculated to  $f(\alpha)$  of the corresponding edge state of the Fibonacci model, and showed that  $f(\alpha_{\min})$  is not zero and  $f(\alpha_{\max})$  is zero for  $\{\bar{1}\bar{1}\bar{1}\bar{1}\bar{1}\bar{1}\dots\}$ . This is contrary to our result of the Harper model.

In Fig. 6(b), we display  $f(\alpha)$  for the center state  $\{0000000\dots\}$ . The values of  $\alpha_{\min}$  and  $\alpha_0$  are 0.358 and 1.31, respectively, and  $f(\alpha_{\min})=0$ . As for  $\alpha_{\max}$  and  $f(\alpha)$  near  $\alpha_{\max}$ , the convergence of our numerical estimate is

rather poor in this case. We roughly estimate that  $\alpha_{\max}\sim 3$  and  $f(\alpha_{\max})\sim 0$ .

Evangelou and Marder<sup>20</sup> have calculated  $f(\alpha)$  for the state  $\{0000000\dots\}$ . Their result is consistent with ours, at least, except for  $\alpha$  near  $\alpha_{\max}$ .

We have calculated  $f(\alpha)$  at  $\lambda=2$  for some other states. In the state  $\{0\bar{1}\bar{1}\bar{1}\bar{1}\bar{1}\bar{1}\dots\}$ , for example,  $\alpha_{\min}$  and  $\alpha_0$  are 0.169 and 1.53, respectively, which are identical to those of  $\{\bar{1}\bar{1}\bar{1}\bar{1}\bar{1}\bar{1}\dots\}$ . Moreover,  $f(\alpha)$  itself is identical in  $\alpha_{\min}\leq\alpha\leq\alpha_0$  for  $\{\bar{1}\bar{1}\bar{1}\bar{1}\bar{1}\bar{1}\dots\}$  and  $\{0\bar{1}\bar{1}\bar{1}\bar{1}\bar{1}\bar{1}\dots\}$ . In general, all of the "edge states" have identical values of  $\alpha_{\min}$  ( $=0.169$ ) and  $\alpha_0$  ( $=1.53$ ), and have identical  $f(\alpha)$

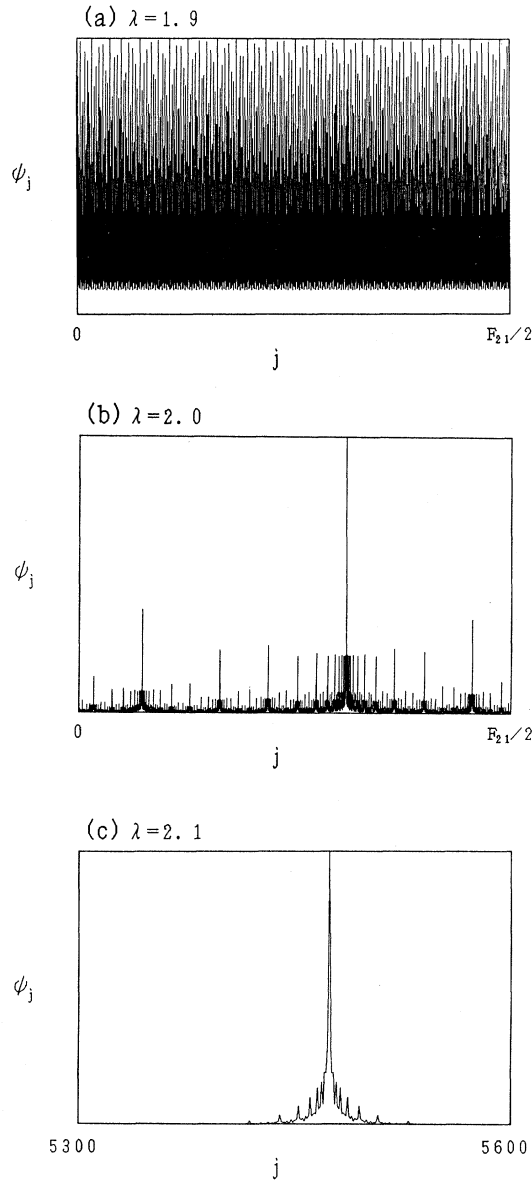


FIG. 2. The wave function  $\{\psi_j\}$  of the state  $\{\bar{1}\bar{1}\bar{1}\bar{1}\bar{1}\bar{1}\dots\}$  for (a)  $\lambda=1.9$ , (b)  $\lambda=2.0$ , and (c)  $\lambda=2.1$ , with  $n=21$  ( $F_{21}=17711$ ). Here  $\psi_j$  is depicted only for  $0\leq j\leq F_{21}/2$  since the wave function is symmetric with respect to the site  $j=0$ .

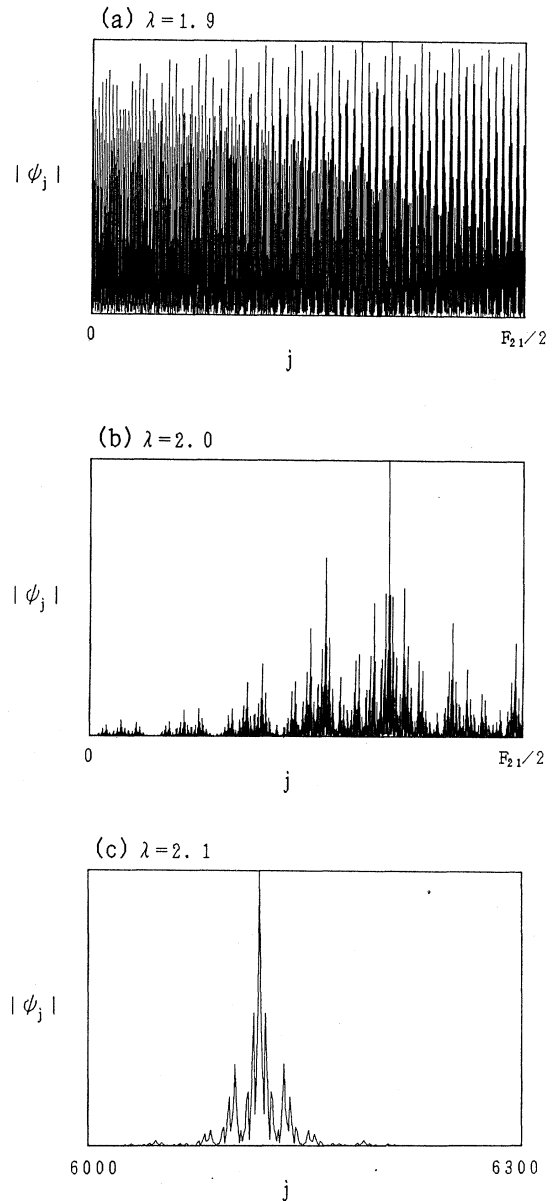


FIG. 3. The magnitude of the wave function of the state  $\{000000\dots\}$  for (a)  $\lambda=1.9$ , (b)  $\lambda=2.0$ , and (c)  $\lambda=2.1$ , with  $n=21$  ( $F_{21}=17711$ ).

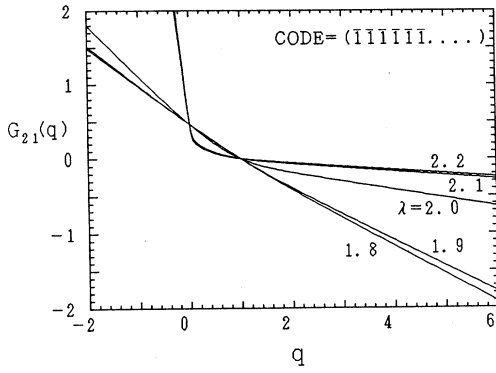


FIG. 4. The “free energy”  $G_n(q)$  ( $n=21$ ) for the wave function of the state  $\{111111\cdots\}$  when  $\lambda=1.8, 1.9, 2.0, 2.1,$  and  $2.2$ . A sharp transition at  $\lambda=2.0$  is observed.

in  $\alpha_{\min} \leq \alpha \leq \alpha_0$ . In the same way, all of the “center states” have identical values of  $\alpha_{\min}$  ( $=0.385$ ) and  $\alpha_0$  ( $=1.31$ ), and have identical  $f(\alpha)$  in  $\alpha_{\min} \leq \alpha \leq \alpha_0$ .

On the other hand, it is harder to have qualitative results on  $\alpha_{\max}$  and  $f(\alpha)$  for  $\alpha \gtrsim \alpha_0$ , since in our calculation ( $n \leq 27$ ), we cannot estimate reliably the  $n \rightarrow \infty$  results, except for the states  $\{00000\cdots\}$  and  $\{11111\cdots\}$ . However, in view of the possible existence of the renormalization-group structure, we can conjecture that

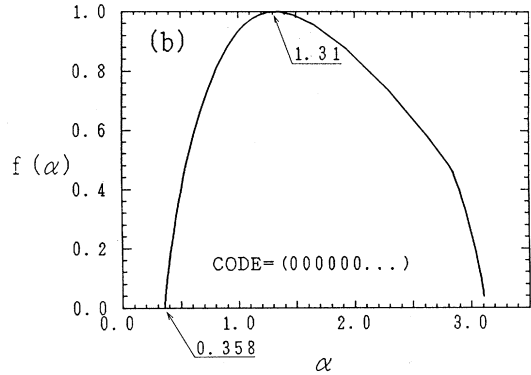
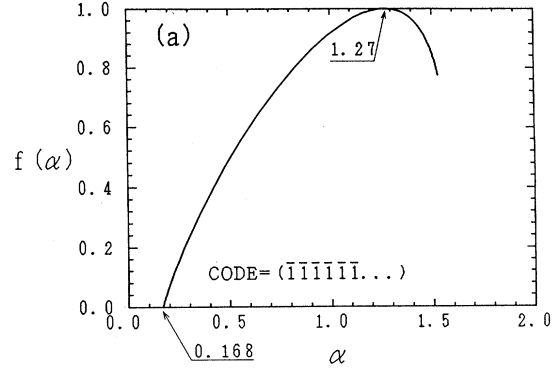


FIG. 6. Plots of the singular spectrum  $f(\alpha)$  for the wave functions (a)  $\{111111\cdots\}$  and (b)  $\{000000\cdots\}$  at the critical case ( $\lambda=2$ ).

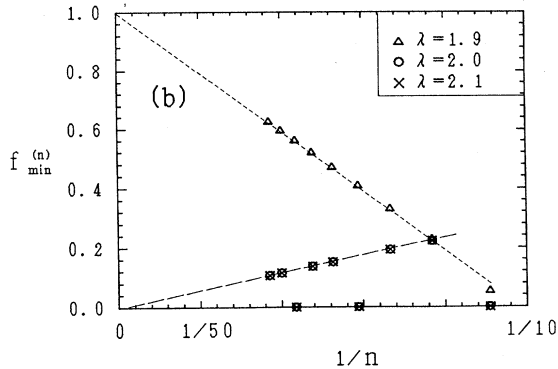
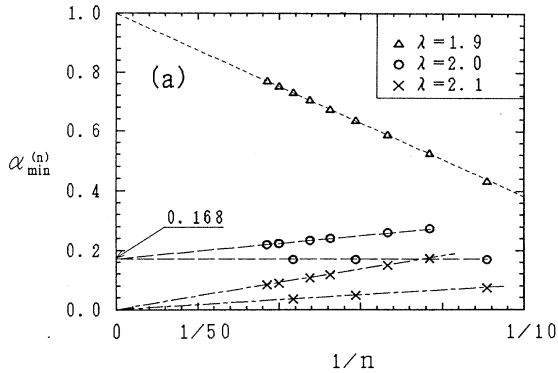


FIG. 5. Plots of (a)  $\alpha_{\min}^{(n)}$  and (b)  $f_{\min}^{(n)}$  against  $1/n$ .

$f(\alpha)$  would be universal in the whole range of  $[\alpha_{\min}, \alpha_{\max}]$  for the “edge states” and “center states”, respectively.

In this section, we have applied the bandwidth analysis and the wave-function analysis to the Harper model, and have demonstrated that both the methods are very effective means to distinguish extended, localized, and critical states. In the critical case of the Harper model ( $\lambda=2$ ), in addition, we have first explicitly shown that  $f(\alpha)$  of a wave function (at least for  $\alpha \lesssim \alpha_0$ ) and the spectrum scaling index  $\gamma$  are universal both for the “edge states” and for the “center states.”

#### IV. GENERALIZED HARPHER MODEL

In this section, we study a model in which  $V(x)$  has two Fourier components:

$$V(x) = \lambda_1 \cos(2\pi x) + \lambda_m \cos(2m\pi x), \quad (22)$$

where  $m$  is an integer ( $m \geq 2$ ). This model, in fact, relates to the problem of an electron under a magnetic field in a three-dimensional lattice.<sup>24</sup> A similar model has been studied previously by other workers,<sup>4,10,11</sup> and the existence of mobility edges has been pointed out. These studies, however, are not systematic numerical studies, and the precise mobility-edge structure has not been well

understood. In fact, Aubry and André<sup>4</sup> suggest that infinitely many mobility edges exist, while Soukoulis and Economou<sup>10</sup> claim that only one mobility edge exists. Chao *et al.*<sup>11</sup> say that several mobility edges are found.

On the other hand, there is a theorem due to Herman:<sup>25</sup> when  $V(x) = \sum_{p=1}^n \lambda_p \cos(2\pi px)$ , the Lyapunov exponent  $\gamma(E)$  satisfies the inequality  $\gamma(E) < \ln(|\lambda_n|/2)$  for almost every  $\omega$  and  $\theta$ . That is, if  $|\lambda_n| > 2$ , the Lyapunov exponent  $\gamma(E) > 0$ , irrespective of  $E$ ; thus all the states are exponentially localized. Therefore, for the model defined by Eq. (22), the spectrum is purely dense point if  $|\lambda_m| > 2$ . However, this theorem gives us no information about the properties for  $|\lambda_m| \leq 2$ , where the spectrum may be nonpure and mobility edges may exist.

Hereafter, we study the case of  $m = 3$ . Then a relation  $V(x + \frac{1}{2}) = -V(x)$  holds as in the Harper model; thus, in the incommensurate limit, the spectrum is symmetric with respect to  $E = 0$ . For  $m = 2$ , for example, this is not the case. In the following calculation, we take  $\omega$  to be  $\sigma \equiv (\sqrt{5} - 1)/2$  and  $\theta$  to be 0, as in the previous section. Thus each state can be specified by an infinite sequence of 1, 0, and  $\bar{1}$ . Applying the methods mentioned in the preceding sections, we explore the properties of this model in detail. Special attention is paid to clarifying the mobility-edge structure of the nonpure spectrum.

When  $\lambda_1 = 0$  or  $\lambda_3 = 0$ , this model (the generalized Harper model) reduces to the ordinary Harper model. Thus if  $\lambda_1 > 2$  ( $\lambda_1 < 2$ ) and  $\lambda_3 = 0$ , all the states are localized (extended). If also  $\lambda_3 > 2$  ( $\lambda_3 < 2$ ) and  $\lambda_1 = 0$ , all the states are localized (extended). In the general case ( $\lambda_1 \neq 0$  and  $\lambda_3 \neq 0$ ), localized and extended states may coexist. First we show in Fig. 7 the phase diagram of this model. The concrete numerical data from which we obtained this phase diagram will be presented in the latter part of this section. When  $\lambda_1$  and  $\lambda_3$  are sufficiently large, all the states are localized (region I). When  $\lambda_1$  and  $\lambda_3$  are small, all the states are extended (region II). In the intermediate values of  $\lambda_1$  and  $\lambda_3$ , the spectrum is nonpure, and localized and extended states coexist (region III). We find no critical state except when  $(\lambda_1, \lambda_3)$  is (2,0) or (0,2). As shown below, a finite number of mobility edges exist in region III. Note that all the states are localized for  $\lambda_3 > 2$  on this phase diagram. This is consistent with the Herman's theorem, mentioned above.

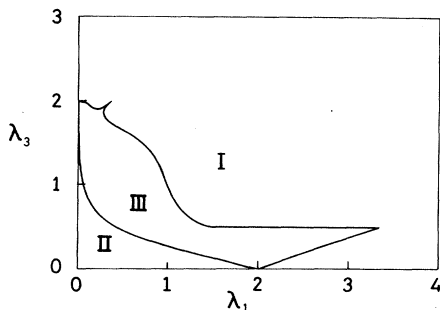


FIG. 7. The phase diagram on the  $\lambda_1$ - $\lambda_3$  plane. There is a remarkable discontinuity at  $\lambda_3 = 0.25$ .

In the phase diagram, there are several features: the boundary between I and III is parallel to the  $\lambda_1$  axis at  $\lambda_3 = 0.5$ . When  $1.5 < \lambda_1 < 3.3$ , all the states are localized at  $\lambda_3 = 0.5$ , while extended states appear for smaller  $\lambda_3$ , no matter how close to 0.5. Another feature found in this diagram is a small dip near  $(\lambda_1, \lambda_3) = (0, 2)$ . These features are probably due to the speciality that  $V(x)$  has only two Fourier components. In fact, the model (5), which has an infinite number of Fourier components, does not show such an awkward behavior.<sup>12</sup>

In the following part of this section, we show the details of numerical analyses, and clarify the precise mobility-edge structure of the nonpure spectrum in the generalized Harper model. First we show an example of the bandwidth analysis in this model. Figure 8 is a plot of  $n$  versus  $F_n B_n$  for several states when  $\lambda_1 = 2.0$  and  $\lambda_3 = 0.25$ . It is clearly seen that the states specified by  $\{\bar{1}\bar{1}\bar{1}\bar{1}\bar{1}\dots\}$ ,  $\{\bar{1}0000\dots\}$ , and  $\{\bar{1}1111\dots\}$  are localized, whereas the states specified by  $\{00000\dots\}$  and  $\{0\bar{1}\bar{1}\bar{1}\bar{1}\dots\}$  are extended. By applying the same analysis to other states, we can see that all the states specified by  $\{0\dots\}$  are extended and all the states specified by  $\{1\dots\}$  or  $\{\bar{1}\dots\}$  are localized. Thus the spectrum has two mobility edges located in the gap between the states  $\{0\bar{1}\bar{1}\bar{1}\bar{1}\dots\}$  and  $\{\bar{1}1111\dots\}$  and in the gap between the states  $\{01111\dots\}$  and  $\{\bar{1}\bar{1}\bar{1}\bar{1}\dots\}$ .

Next we show an example of the wave-function analysis. The case of  $\lambda_1 = 2.0$  and  $\lambda_3 = 0.25$  is studied as the above. Figure 9 is a plot of  $1/n$  versus (a)  $\alpha_{\min}^{(n)}$ , (b)  $f_{\min}^{(n)}$ , and for  $\{0\bar{1}\bar{1}\bar{1}\bar{1}\dots\}$  and  $\{\bar{1}1111\dots\}$ . It is found that  $\alpha_{\min} = \lim_{n \rightarrow \infty} \alpha_{\min}^{(n)} = 1$  and  $f(\alpha_{\min}) = \lim_{n \rightarrow \infty} f_{\min}^{(n)} = 1$  for  $\{0\bar{1}\bar{1}\bar{1}\bar{1}\dots\}$ , while  $\alpha_{\min} = 0$  and  $f(\alpha_{\min}) = 0$  for  $\{\bar{1}1111\dots\}$ . Thus it is concluded that the state  $\{0\bar{1}\bar{1}\bar{1}\bar{1}\dots\}$  is extended and the state  $\{\bar{1}1111\dots\}$  is localized. This is consistent with the result of the bandwidth analysis.

We use both the methods (the bandwidth analysis and the wave-function analysis) to obtain the following data.

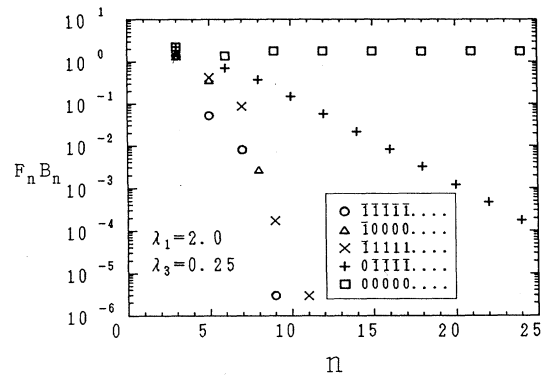


FIG. 8. A plot of  $F_n B_n$  against  $n$  for  $\lambda_1 = 2.0$  and  $\lambda_3 = 0.25$ . The states specified by  $\{\bar{1}\bar{1}\bar{1}\bar{1}\bar{1}\dots\}$ ,  $\{\bar{1}0000\dots\}$ , and  $\{\bar{1}1111\dots\}$  turn out to be localized, while the states specified by  $\{0\bar{1}\bar{1}\bar{1}\bar{1}\dots\}$  and  $\{00000\dots\}$  are extended.

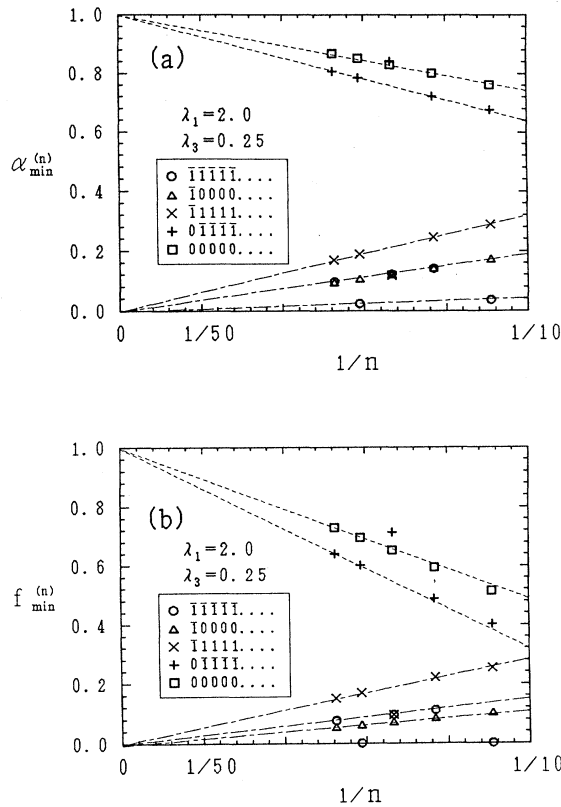


FIG. 9. Plots of (a)  $\alpha_{\min}^{(n)}$  and (b)  $f_{\min}^{(n)}$  against  $1/n$  for  $\lambda_1=2.0$  and  $\lambda_3=0.25$ . Localized and extended states are clearly distinguished as the bandwidth analysis in Fig. 8.

We checked that the two methods always give a consistent result.

Now we show an overall behavior of the spectrum. Figure 10 shows the spectra for various values of  $\lambda_1$  and  $\lambda_3=0.25$  fixed. Only the lower halves of the spectra ( $E < 0$ ) are displayed, since the spectra are symmetric with respect to  $E=0$ . The line in the figure is a mobility edge. In the lower-energy side of the line, the states are localized, while in the upper side, the states are extended. For  $\lambda_1 < \lambda_1^{(c1)}$  ( $\approx 1.04$ ), all the states are extended: the spectrum is purely absolutely continuous. For  $\lambda_1 > \lambda_1^{(c2)}$  ( $\approx 2.66$ ), on the other hand, all the states are localized: the spectrum is pure point. For  $\lambda_1^{(c1)} < \lambda_1 < \lambda_1^{(c2)}$ , the spectrum is nonpure: extended states and localized states coexist in the spectrum. At  $\lambda_1 = \lambda_1^{(c1)}$ , the states of the lowest (highest) energy become localized, and for  $\lambda_1 > \lambda_1^{(c1)}$  the mobility edges appear and divide the spectrum into the two regions: the states in the outer sides of the mobility edges are localized, whereas the states in the inner side are extended. This is analogous to the Anderson localization in the three-dimensional disordered systems, and is in contrast to the behavior found in the model with the potential (5), where the states in the inner side of the mobility edges are localized and the states in the outer sides are extended.<sup>12</sup> The mobility edges move towards the center of the spectrum as  $\lambda_1$  is increased, and

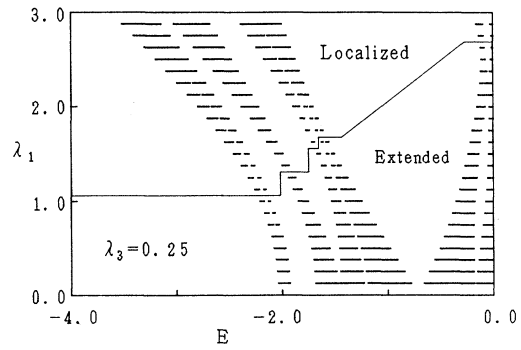


FIG. 10. The energy spectra for various values of  $\lambda_1$  and  $\lambda_3=0.25$ .

finally all the states become localized at  $\lambda_1 = \lambda_1^{(c2)}$ .

In  $\lambda_1^{(c1)} < \lambda_1 < \lambda_1^{(c2)}$ , the mobility edges have a tendency to be located in large gaps in the spectrum. In Fig. 11, we show how the position of a mobility edge moves with  $\lambda_1$  when  $\lambda_3=0.25$ . For  $1.115 < \lambda_1 < 1.310$ , the mobility edge stays in the gap between  $\{111111\cdots\}$  and  $\{101111\cdots\}$ , and for  $1.355 < \lambda_1 < 1.590$ , it stays in the gap between  $\{101111\cdots\}$  and  $\{111111\cdots\}$ . In a rather narrow range  $1.310 < \lambda_1 < 1.355$ , the mobility edge moves between the two large gaps. In most of the range, however, the mobility edge stays in the gap between  $\{10111111\cdots\}$  and  $\{10011111\cdots\}$  and in the gap between  $\{10011111\cdots\}$  and  $\{10111111\cdots\}$ .

By now, we have shown the properties of the system with  $\lambda_3=0.25$ . In that case, the mobility edges have been shown to move from the edges of the spectrum to the center. However, this is not always the case for other values of  $\lambda_3$ . For the states specified by  $\{1C_2C_3C_4\cdots\}$ , the situation changes itself continuously: the mobility edges move from the edges of the spectrum to the center with increasing  $\lambda_1$  when  $\lambda_3$  is fixed, and the values of  $\lambda_1$  where the individual states become localized decrease continuously with increasing  $\lambda_3$ . However, the states specified by  $\{0C_2C_3C_4\cdots\}$  show a very curious behavior. For  $\lambda_3 < 0.5$ , localization starts from  $\{011111\cdots\}$

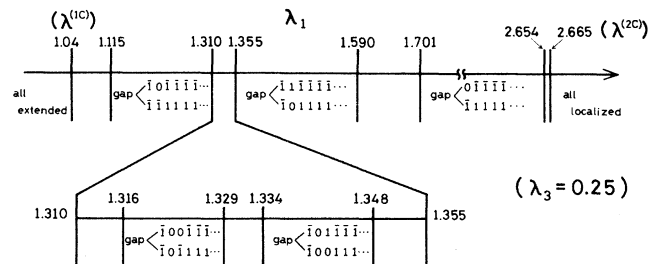


FIG. 11. The location of a mobility edge as a function of  $\lambda_1$  for  $\lambda_3=0.25$ . When  $1.115 < \lambda_1 < 1.310$ , for example, the mobility edge is in the gap between  $\{101111\cdots\}$  and  $\{111111\cdots\}$ . The location has a tendency to stay in large energy gaps, and moves from the edge of the spectrum towards the center as  $\lambda_1$  is increased.



and finally the state  $\{0000 \cdots\}$  becomes localized at  $\lambda_1^{(c2)}$ . The value of  $\lambda_1$  where the state  $\{0\bar{1}\bar{1}\bar{1}\bar{1} \cdots\}$  becomes localized ( $\lambda_1^{(c3)}$ ) and  $\lambda_1^{(c2)}$  are very close to each other (for example,  $\lambda_1^{(c2)}=2.665$  and  $\lambda_1^{(c3)}=2.654$  when  $\lambda_3=0.25$ ). That is, the states specified by  $\{0C_2C_3C_4 \cdots\}$  localize almost at once. The values of  $\lambda_1^{(c2)}$  and  $\lambda_1^{(c3)}$  increase with  $\lambda_3$ . However,  $\lambda_1^{(c2)}$  and  $\lambda_1^{(c3)}$  become smaller discontinuously at  $\lambda_3=0.5$ . For  $\lambda_3 \geq 0.5$ , moreover,  $\lambda_1^{(c2)}$  is smaller than  $\lambda_1^{(c3)}$ : the state  $\{00000 \cdots\}$  becomes localized at a smaller value of  $\lambda_1$  than the state  $\{0\bar{1}\bar{1}\bar{1}\bar{1} \cdots\}$ . A similar situation is also found in another model.<sup>12</sup> The values of  $\lambda_1^{(c2)}$  and  $\lambda_1^{(c3)}$  decrease with increasing  $\lambda_3$  for  $\lambda_3 \geq 0.5$ .

From the above, for  $\lambda_3 < 0.5$ , the boundary between I and III in Fig. 7 is a line where localization of  $\{00000 \cdots\}$  takes place, while for  $\lambda_3 \geq 0.5$  it is a line where localization of  $\{0\bar{1}\bar{1}\bar{1}\bar{1} \cdots\}$  takes place. However, this is not the case in the neighborhood of the dip in Fig. 6: in this region, the boundary is a line where localization of  $\{00000 \cdots\}$  occurs, as in  $\lambda_3 < 0.5$ .

## V. SUMMARY AND CONCLUSIONS

In this paper, we have explained the methods of analyzing the spectrum and the wave functions of one-dimensional discrete Schrödinger equations with a quasiperiodic potential. The methods have been applied to the Harper model and the generalized Harper model [Eq. (20)].

The results obtained from both methods are consistent with each other, as expected. Thus we can clearly distinguish localized, extended, and critical states, and can study the scaling properties of the critical states.

For the Harper model, the well-known conjecture that all the states are extended (localized) for  $\lambda < 2$  ( $\lambda > 2$ ) is confirmed. For the critical case ( $\lambda = 2$ ), some interesting universal behaviors are observed. All the "edges states" specified by  $\{\cdots 11111 \cdots\}$  or  $\{\cdots \bar{1}\bar{1}\bar{1}\bar{1} \cdots\}$  have an identical value of the scaling index of the spectrum ( $\gamma = \gamma_E \equiv 2.374$ ), and all the "center states" specified by  $\{\cdots 00000 \cdots\}$  have an identical index ( $\gamma = \gamma_C \equiv 1.826$ ) as well. Furthermore, this universality appears in the scaling property of the wave functions themselves: all the "edge states" ("center states") have an identical  $f(\alpha)$ , although this is not yet certain near  $\alpha_{\max}$ , where the convergence of our numerical calculation is poor. These behaviors are likely to show the existence of an renormalization-group structure in the Harper model.

For the generalized Harper model (20), extended and localized states coexist in the spectrum. The regions of the localized and the extended states in the spectrum are separated by mobility edges. When  $\lambda_3$  is fixed and  $\lambda_1$  is increased from zero, localization starts from the edge of the spectrum at a value of  $\lambda_1$ , and the mobility edges move from the edges of the spectrum towards the center of the spectrum. After the localization of the states in the outer bands specified by  $\{1 \cdots\}$  or  $\{\bar{1} \cdots\}$  has completed, the localization of the center band corresponding to the states specified by  $\{0 \cdots\}$  takes place. For  $\lambda_3 < 0.5$ , the states of this band localize from the edges to the center. On the other hand, for  $\lambda_3 \geq 0.5$ , the states of the center band localize from the center to the edge.

The mobility edges stay in large gaps for most of the values of  $\lambda_1$  and  $\lambda_3$ . In other words, the mobility edges are located more probably in gaps belonging to upper levels of the hierarchical band structure (tree structure) than in those belonging to lower levels. In any case, the mobility edges always stay in gaps; thus there is no critical state in the generalized Harper model except at the two points  $(\lambda_1, \lambda_3) = (2, 0)$  and  $(\lambda_1, \lambda_3) = (0, 2)$  on the  $\lambda_1$ - $\lambda_3$  plane. Critical states (singular continuous spectrum) appear only at very special situations, and are unstable against some perturbations.

In this paper and in Ref. 12, we have studied one-dimensional QP systems with nonpure spectra. Although we have found completely unexpected and exotic properties in such systems, the spectra are in any case separated into dense point and absolutely continuous regions by finite numbers of mobility edges.

One of the other possibilities of the structure of the nonpure spectrum is that there would be infinitely many mobility edges. The one-dimensional QP systems have an infinite hierarchical structure of subbands. Thus there is a possibility of the hierarchy of the mobility-edge structure. However, the models we studied do not exhibit such a behavior.

## ACKNOWLEDGMENTS

This work was partly supported by a Grant-in-Aid for Scientific Research from the Ministry of Education, Science and Culture, Japan. We had useful discussions with S. Aubry, T. Spencer, and H. Tsunetsugu. One of us (M.K.) was, in part, supported by the U.S. National Science Foundation under Grant No. DMR-86-15609 and by the Alfred P. Sloan Foundation (New York, N.Y.).

<sup>1</sup>See, for example, J. B. Sokoloff, Phys. Rep. **126**, 189 (1985).

<sup>2</sup>P. G. Harper, Proc. Phys. Soc. London, Sect. A **68**, 874 (1955).

<sup>3</sup>D. R. Hofstadter, Phys. Rev. B **14**, 2239 (1976).

<sup>4</sup>A. Aubry and G. André, Ann. Isr. Phys. Soc. **3**, 133 (1980).

<sup>5</sup>M. Kohmoto, Phys. Rev. Lett. **51**, 1198 (1983).

<sup>6</sup>S. Ostlund and R. Pandit, Phys. Rev. B **29**, 1394 (1984).

<sup>7</sup>D. R. Grempell, S. Fishman, and R. Prange, Phys. Rev. Lett. **49**, 833 (1982).

<sup>8</sup>M. Kohmoto, L. P. Kadanoff, and C. Tang, Phys. Rev. Lett.

**50**, 1870 (1983).

<sup>9</sup>S. Ostlund, R. Pandit, D. Rand, H. J. Shellnhuber, and E. D. Siggia, Phys. Rev. Lett. **50**, 1873 (1983).

<sup>10</sup>C. M. Soukoulis and E. N. Economou, Phys. Rev. Lett. **48**, 1043 (1982).

<sup>11</sup>K. A. Chao, R. Riklund, and Y. L. Liu, Phys. Rev. B **32**, 5979 (1985); Y. L. Liu, R. Riklund, and K. A. Chao, *ibid.* **32**, 8385 (1986); Y. L. Liu and K. A. Chao, *ibid.* **34**, 5247 (1986).

<sup>12</sup>H. Hiramoto and M. Kohmoto, Phys. Rev. Lett. **62**, 2714

- (1989).
- <sup>13</sup>C. Tang and M. Kohmoto, Phys. Rev. B **34**, 2041 (1986).
- <sup>14</sup>M. Kohmoto and Y. Oono, Phys. Lett. **102A**, 145 (1984).
- <sup>15</sup>M. Kohmoto, B. Sutherland, and C. Tang, Phys. Rev. B **35**, 1020 (1987).
- <sup>16</sup>T. C. Halsey, M. H. Jensen, L. P. Kadanoff, I. Procaccia, and B. I. Shraiman, Phys. Rev. A **33**, 1141 (1986).
- <sup>17</sup>T. Janssen and M. Kohmoto, Phys. Rev. B **38**, 5811 (1988).
- <sup>18</sup>A. P. Siebesma and L. Pietronero, Europhys. Lett. **4**, 587 (1987).
- <sup>19</sup>S. N. Evangelou, J. Phys. C **20**, L295 (1987).
- <sup>20</sup>S. N. Evangelou and M. Marder (unpublished).
- <sup>21</sup>T. Fujiwara, M. Kohmoto, and T. Tokihiro, Phys. Rev. B **40**, 7413 (1989).
- <sup>22</sup>M. Kohmoto, Phys. Rev. A **37**, 1345 (1988).
- <sup>23</sup>The index  $\beta$  defined by H. Hiramoto and S. Abe [J. Phys. Soc. Jpn. **57**, 1365 (1988)] is, in fact, identical to  $\alpha_{\min}/2$ . The value of  $\beta$  calculated there is 0.084.
- <sup>24</sup>G. Montambaux and M. Kohmoto (unpublished).
- <sup>25</sup>M. Herman, Commun. Math. Helv. **58**, 453 (1983).